Inflammation Research (2026) 75:97
https://doi.org/10.1007/s00011-026-02245-2

Inflammation Research

RESEARCH

Tm4sf19 inhibition alleviates imiquimod-induced psoriatic dermatitis by regulating inflammatory signaling pathways and keratinocyte proliferation in mice

Min Gi Kang[1] · Sujin Park[1] · Eunji Hong[1] · Min-Jung Lee[2] · Da Seul Jung[1] · Jin Sun Heo[1] · Haein An[1] · Min Woo Kim[2] · Naim Park[2] · Hyeyeon Park[1,3] · Pyunggang Kim[1] · Minjung Son[1,3] · Kyoungwha Pang[1] · Jinah Park[1] · Ga-Eun Hwang[1] · Yong Jung Kwon[1] · Seiya Mizuno[4] · Satoru Takahashi[5] · Seok Hee Park[3] · Seong-Jin Kim[1,2]

Received: 31 October 2025 / Revised: 2 April 2026 / Accepted: 5 April 2026

Abstract

Background Psoriasis is a chronic inflammatory disease characterized by keratinocyte hyperproliferation, immune cell infiltration, and persistent inflammatory signaling. Although Tm4sf19 has been implicated in inflammatory processes, its contribution to psoriasis pathogenesis remains unclear.

Methods We investigate the role of Tm4sf19 in psoriatic inflammation was examined using an imiquimod-induced psoriasis mouse model and HaCaT keratinocytes, in which Tm4sf19 expression was deleted genetically or suppressed pharmacologically with the competitive inhibitor, LEL-Fc. Gene expression, protein expression, and tissue changes were assessed by qPCR, western blotting and histological scoring, respectively.

Results Tm4sf19 expression was significantly elevated in psoriatic lesion. Tm4sf19 knockout or inhibition using LEL-Fc suppressed psoriatic symptoms, macrophage-mediated inflammation and inflammatory cytokine expression. Tm4sf19 inhibition also suppressed the activation of STAT3, EGFR, ERK and KRT17 signaling pathways in keratinocytes. Furthermore, LEL-Fc treatment effectively inhibited LPS-induced cell cycle progression and promoted apoptosis in keratinocyte both in vivo and in vitro.

Conclusion These findings suggest that Tm4sf19 regulates psoriatic inflammation and keratinocyte proliferation through major signaling pathways. Therefore, inhibiting Tm4sf19 may have therapeutic potential for the treatment of psoriasis.

Keywords Imiquimod-induced psoriasis murine model · Macrophage · Keratinocyte apoptosis · Competitive inhibitor · EGFR

Responsible Editor: John Di Battista.

✉ Sujin Park
sujinpark@gilo.or.kr

✉ Seong-Jin Kim
jasonsjkim@gilo.or.kr

1 GILO Institute, GILO Foundation, 92 Myeongdal-ro, Seocho-gu, Seoul 06668, Republic of Korea

2 Medpacto Inc., Seoul, Republic of Korea

3 Department of Biological Sciences, Sungkyunkwan University, Suwon, Republic of Korea

4 Laboratory Animal Resource Center in Transborder Medical Research Center, Institute of Medicine, University of Tsukuba, Tsukuba, Japan

5 Department of Anatomy and Embryology, Faculty of Medicine, University of Tsukuba, Tsukuba, Japan

Introduction

Psoriasis is a chronic, immune-mediated inflammatory skin disorder characterized by excessive keratinocyte proliferation, infiltration of immune cells, and sustained activation of inflammatory signaling cascades [1–3]. The process involves complicated interactions among keratinocytes, immune cells, and pro-inflammatory cytokines, ultimately leading to the development of distinctive erythematous plaques [4]. Keratinocytes play a central role in the pathogenesis of psoriasis, not only as passive targets of inflammation but also as active participants by producing pro-inflammatory cytokines and chemokines that perpetuate the inflammatory cycle [5]. Macrophages are essential for regulating immunological responses and their role in

Published online: 17 April 2026

the pathophysiology of psoriasis is increasingly being recognized [6, 7]. In psoriasis, macrophages are stimulated to secrete pro-inflammatory cytokines, including TNF-α, IL-6, and IL-1β, which enhance the inflammatory response [8].

Tetraspanins are a family of transmembrane proteins that have two extracellular loops and four alpha-helical transmembrane domains. Tetraspanins are known to be essential for immune responses and interactions between cells [9, 10]. Transmembrane superfamily 4 (TM4SF) is known to be involved in various cellular functions, including cell adhesion, migration, apoptosis, differentiation, proliferation, and signal transduction [11, 12]. In a previous study, we demonstrated that inhibition of Tm4sf19 suppressed pro-inflammatory responses in macrophages [13]. This finding suggested that Tm4sf19 may be involved in psoriatic skin inflammation. Therefore, we examined whether Tm4sf19 contributes not only to psoriatic inflammation but also to keratinocyte activation. To address this, the role of Tm4sf19 was investigated using knockout (KO) mice and LEL-Fc, a competitive inhibitor comprising the large extracellular loop of Tm4sf19 fused to hIgG1 in an imiquimod-induced psoriasis model [14].

Material and methods

Ethical statements

Mice were housed at the MedPacto Animal Care Center under specific pathogen-free conditions. All animal research received approval from the Institutional Animal Care and Use Committee at MedPacto Animal Care Center (Approval No. 2023-0001) and performed following the ARRIVE guidelines and the above ethical approval.

Animal models

Eight-week-old female WT and Tm4sf19 KO mice, derived from a C57BL/6 background, were generated as described previously [14]. Mice were shaved on their dorsal skin and subjected to daily topical application of 62.5 mg of 5% Imiquimod (IMQ) cream (DONG-A ST, Korea) for four consecutive days to generate psoriasis-like skin inflammation. Control mice were received Vaseline instead of IMQ under equivalent settings. Concurrently with the daily IMQ application, 50 mg/kg of LEL-Fc was administered intravenously (i.v.) via the tail vein to evaluate its therapeutic effect. Body weight and back skin thickness measurements and assessments for redness and scaling were also performed daily throughout the treatment period. At the end of the treatment period, mice were euthanized, and dorsal skin tissues and spleens were collected.

Cell culture

RAW264.7 macrophages, HaCaT keratinocytes and HEK293T cells were cultured in Dulbecco's Modified Eagle Medium (DMEM) enriched with 10% fetal bovine serum (FBS) and 1% penicillin–streptomycin at 37 °C in a 5% CO_2 environment.

Bone marrow-derived macrophages (BMDMs) were derived from WT and Tm4sf19 KO mice and cultured in DMEM supplemented with 10% FBS and 20 ng/mL macrophage colony-stimulating factors (M-CSF) for 7 days to promote macrophage differentiation.

Cells were pre-treated with the LEL-Fc fusion protein at a concentration of 50 μg/ml, unless otherwise indicated, for 2–4 h prior to stimulation with 4 μg/ml of IMQ for the indicated time points.

Antibodies

Following antibodies were used: anti-β actin (A5441, Sigma Aldrich), anti-α tubulin (T5168, Sigma Aldrich), anti-IL-17A (ab79056, Abcam), anti-IL-6 (ab290735, Abcam), anti-IL-1β (ab9722, Abcam), anti-TNF-α (ab6671, Abcam; sc-52746, Santa Cruz Biotechnology), anti-MYD88 (sc-74532, Santa Cruz Biotechnology), anti-COX2 (35–8200, Thermo Fisher), anti-phospho p65 (pp65) (3033S, Cell Signaling Technology), anti-p65 (8242S, Cell Signaling Technology), anti-Caspase9 (9508 T, Cell Signaling Technology), anti-phospho STAT3 (pSTAT3) (9361S, Cell Signaling Technology), anti-STAT3 (5397, Cell Signaling Technology), anti-EGFR (D38B1, Cell Signaling Technology), anti-KRT17 (D73C7, Cell Signaling Technology), anti-phospho p38 (pp38) (9211S, Cell Signaling Technology), anti-p38 (9212S, Cell Signaling Technology), anti-phospho JNK (pJNK) (4668 T, Cell Signaling Technology), anti-JNK (9252S, Cell Signaling Technology), anti-phospho ERK (9101S, Cell Signaling Technology), and anti-ERK (91,028, Cell Signaling Technology), anti-iNOS (ab178945, Abcam), anti-F4/80 (sc-377009, Santa Cruz Biotechnology), anti-NLRP3 (15,101, Cell Signaling Technology), anti-Tm4sf19 (customized), anti-phospho IκBα (14D4, Cell Signaling Technology), anti-CDK2 (2546, Cell Signaling Technology), anti-CDK4 (sc-260, Santa Cruz Biotechnology), anti-HA (sc-7392, Santa Cruz Biotechnology) All antibodies were used at the indicated dilution factors according to the manufacturer's recommendations.

Histological analysis

For histological and immunohistochemical analysis, mouse skin tissues were fixed in 10% paraformaldehyde, dehydrated using a graded alcohol series at room temperature,

and embedded in paraffin. Serial sections with a thickness of 7 μm were prepared. For histological evaluation, the sections were stained with hematoxylin (Sigma, USA) for nuclear visualization and eosin (Sigma, USA) for cytoplasmic staining. For immunohistochemistry (IHC), tissue sections were incubated with primary antibodies to assess inflammatory markers and cellular proliferation. For immunofluorescence (IF) staining, sections were incubated with indicated antibodies and Alexa Fluor 488, 647 antibodies followed by counterstaining with DAPI. Images were acquired using Axio Scan.Z1 (Zeiss) fluorescence slide scanner.

To detect apoptotic cells in skin tissues, a TUNEL (terminal deoxynucleotidyl transferase dUTP nick end labeling) assay was performed using a commercial kit (Roche, 4810–30-K) according to the manufacturer's instructions. After permeabilization with proteinase K (20 μg/mL) for 15 min at room temperature, sections were incubated with TUNEL reaction mixture containing terminal deoxynucleotidyl transferase (TdT) and labeled nucleotides for 60 min at 37 °C in a humidified chamber. Signal was detected using the HRP-conjugated converter and DAB substrate solution. Hematoxylin was used for nuclear counterstaining. TUNEL-positive cells were visualized under a bright-field microscope and quantified in five randomly selected high-power fields per section.

Western blot and immunoprecipitation

Mouse dorsal skin tissues or cells were lysed in RIPA buffer containing protease and phosphatase inhibitors. Protein concentrations were measured using the BCA assay, and samples were separated by SDS-PAGE and transferred to PVDF membranes. After blocking, membranes were incubated with indicated primary and HRP-conjugated secondary antibodies, and signals were detected using the AI600 system. For immunoprecipitation, lysates were incubated overnight with the indicated antibodies, followed by incubation with Dynabeads™ Protein G. The precipitated proteins were analyzed by western blot.

Real-time quantitative PCR (RT-PCR) analysis

Total RNA was extracted from mouse skin tissues using the easy-BLUE Total RNA Extraction Kit (Promega, Cat. No. 17061), following the manufacturer's instructions. The concentration and purity of RNA were assessed using a Nanodrop spectrophotometer. For reverse transcription, M-MLV Reverse Transcriptase (Promega, Cat. No. M1705) was used with 2 μg of total RNA to synthesize complementary DNA (cDNA). The synthesized cDNA was subjected to quantitative RT-PCR (qRT-PCR) using a QuantStudio 5 Real-Time PCR instrument (Applied Biosystems) with TOPreal qPCR 2X PreMIX (Enzynomics, Cat. No. RT500M). Gene expression levels were analyzed using the Ct method, and all target gene expressions were normalized to Gapdh as an internal control.

Flow cytometry analysis

Flow cytometry analyses were conducted to assess both apoptotic cell populations and cell cycle progression. For apoptosis detection, cells were stained with FITC-conjugated Annexin V and propidium iodide (PI) using the Annexin V Apoptosis Detection Kit I (BD Biosciences, USA), according to the manufacturer's protocol. For cell cycle analysis, cells were stimulated with lipopolysaccharide (LPS) with or without pre-treatment with LEL-Fc. Harvested cells were fixed with 70% ethanol, treated with RNase A and incubated with PI (10 μg/mL) for 30 min in the dark at room temperature. Samples were analyzed on a BD FACS Canto II flow cytometer and analyzed by FlowJo software.

Statistical analysis

All experiments were conducted in at least triplicate. Data are presented as the mean ± SD. Prior to statistical comparisons, data normality was assessed using the Shapiro–Wilk test. Statistical significance was determined using either Student's t-test or a one- or two-way ANOVA, followed by Tukey's post hoc test for multiple comparisons, as appropriate. All statistical analyses were performed using GraphPad Prism 8.3 (GraphPad Software, USA).

Results

The expression of Tm4sf19 is elevated in psoriatic conditions

We examined the increased expression of the *tm4sf19* gene in the skin of psoriasis patients compared to healthy normal skin in public data sets (GSE54456) and single-cell transcriptomic analysis (Fig. 1a and Supplementary Fig. 1) [15–18]. To investigate the role of Tm4sf19 in psoriasis, we used an IMQ-induced psoriatic mice model, mimics human psoriatic symptoms. We found that the gene expression of *tnf-α, il-6* and *tm4sf19* was significantly increased in the dorsal skin of IMQ-treated mice compared to Vaseline-treated mice (Fig. 1b). We also demonstrated that the protein expression of Tm4sf19, along with TNF-α, IL-6 and IL-17A, was significantly higher in the dorsal skin of IMQ-treated mice than Vaseline-treated mice (Fig. 1c). In addition, immunofluorescence staining showed that Tm4sf19 expression was increased in epidermis and dermis of

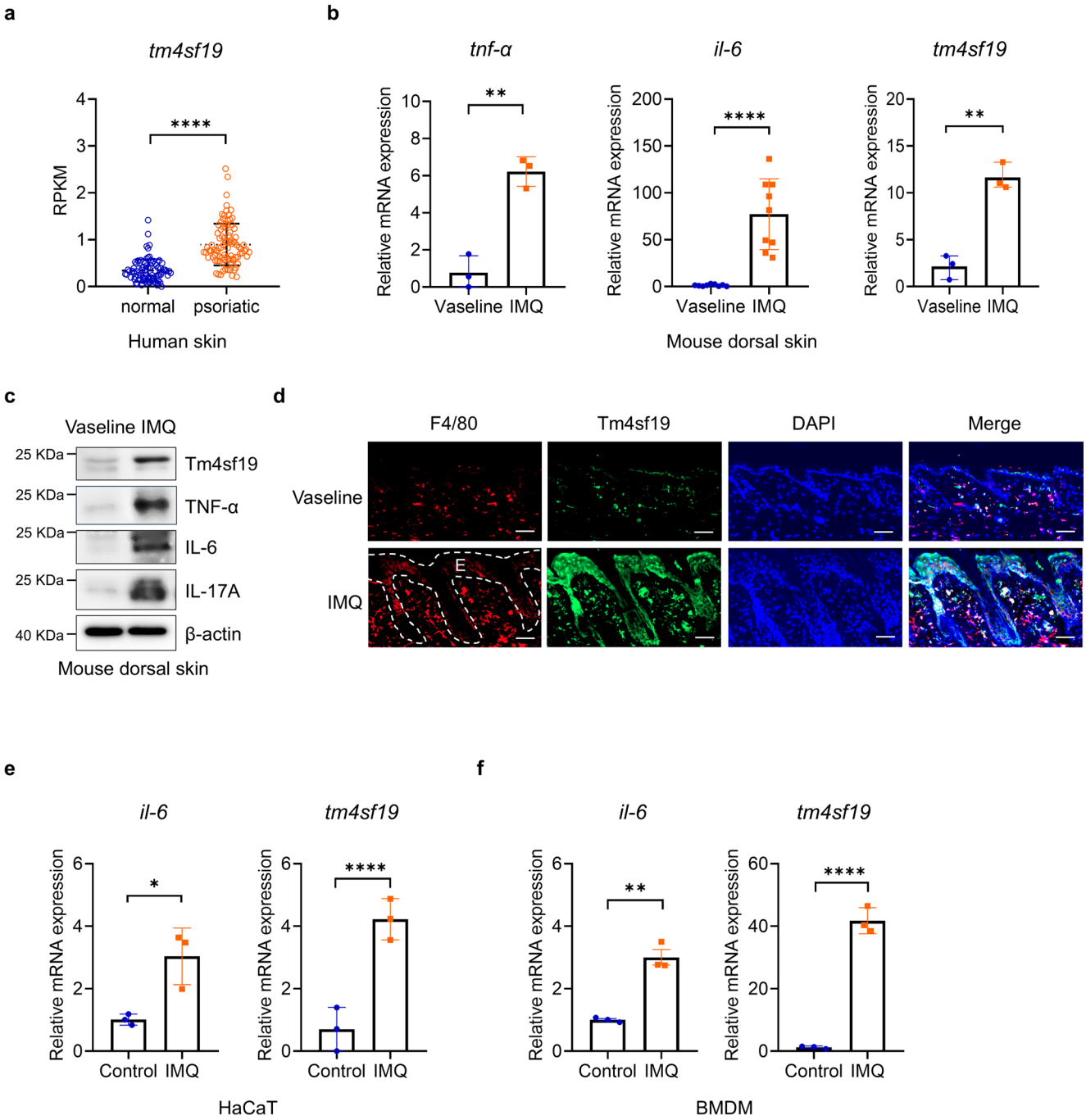

Fig. 1 Tm4sf19 expression is elevated in psoriatic skin and correlates with inflammatory cytokine production. **a** Tm4sf19 expression levels in normal and psoriatic human skin samples from the GSE54456 dataset. **b** Quantitative PCR analysis of *tm4sf19* and marker genes in back skin tissues from Vaseline- or IMQ-treated mice. **c** Western blot analysis of Tm4sf19, and marker protein levels in mouse back skin. **d** Immunofluorescence staining of F4/80 and Tm4sf19 in Vaseline- or IMQ-treated mouse skin. DAPI was indicated nuclear staining. The white dashed line indicates the epidermis area marked E. Scale bar = 50 μm. **e, f** Relative mRNA expression of *il-6* and *tm4sf19* in IMQ-treated HaCaT cells (e) and BMDMs (f). Data are expressed as mean ± SD. *$p<0.05$, **$p<0.01$, ****$p<0.0001$

psoriatic skin of IMQ-treated mice compared with Vaseline-treated skin (Fig. 1d). Furthermore, a significant increase of *il-6* and *tm4sf19* by IMQ treatment in HaCaT keratinocytes and bone marrow-derived macrophages (BMDMs) (Fig. 1e, f). These results suggest that Tm4sf19 plays an important role in psoriasis by regulating pro-inflammatory cytokine production and immune cell activation in keratinocytes and macrophages.

Tm4sf19 deficiency suppresses inflammatory responses in IMQ-induced psoriasis mouse model

To investigate the role of Tm4sf19 in psoriasis, we induced a psoriasis-like phenotype using IMQ treatment in wild-type (WT) and Tm4sf19 KO mice [14]. IMQ-treated WT mice demonstrated significant skin thickening and erythema, typical of psoriatic inflammation; while these symptoms decreased significantly in KO mice (Fig. 2a). Body weight decreased significantly in IMQ-treated group compared to Vaseline-treated group. However, KO mice showed significantly less weight loss than WT during IMQ treatment (Fig. 2b). The Psoriasis Area and Severity Index (PASI) is a widely used clinical measure to assess the severity and extent of psoriatic lesions. It incorporates assessments of redness, scaling, skin thickness, and the affected area to provide a comprehensive evaluation of disease severity [19]. PASI scores were significantly lower in KO mice that WT mice in response to IMQ treatment (Fig. 2c and Supplementary Fig. 2a). We found that quantified skin thickness changes which can assess the extent of epidermal hyperplasia due to IMQ treatment were significantly reduced in KO mice compared to WT mice (Supplementary Fig. 2b). Spleen size and weight, indicators of systemic inflammation, were notably increased in WT mice after IMQ induction but were significantly reduced in KO mice (Fig. 2d, e). Histological analysis using H&E staining demonstrated that the epidermal thickness of KO mice was significantly decreased compared to WT mice after IMQ treatment (Fig. 2f, g). The IHC analysis revealed that the number of TNF-α, IL-1β, and IL-17A-positive cells in the epidermis and dermis was significantly increased following IMQ treatment and it was significantly decreased in IMQ-treated KO mice compared to IMQ-treated WT mice (Fig. 2f, h). These results suggest that deficiency of Tm4sf19 inhibited pro-inflammatory cytokine production and immune responses in psoriasis.

Administration of LEL-Fc, a competitive inhibitor of Tm4sf19, decreases IMQ-induced psoriatic skin inflammation and reduces pro-inflammatory cytokine expression

Based on the result that Tm4sf19 deficiency ameliorates IMQ-induced psoriasis, we investigated whether LEL-Fc (the large extracellular loop domain of Tm4sf19 fused to hIgG1), a competitive inhibitor of Tm4sf19, alleviates IMQ-induced psoriasis. In a previous study, we demonstrated that LEL-Fc effectively suppresses inflammatory responses, suggesting that LEL-Fc is a potential therapeutic agent for inflammatory diseases [13]. To assess the therapeutic efficacy of LEL-Fc in IMQ-induced psoriatic dermatitis, we treated mice with Vehicle, hIgG1 or LEL-Fc in IMQ-induced psoriasis mouse model. Vehicle- and hIgG1-treated groups demonstrated significantly increased skin thickness, scaling and erythema, indicative of psoriatic inflammation, while these symptoms were suppressed in LEL-Fc-treated group in IMQ-induced psoriasis mice (Fig. 3a). Significant body weight loss was observed in the Vehicle- and hIgG1-treated groups, which was suppressed by LEL-Fc treatment in IMQ-treated groups (Fig. 3b). PASI scores were significantly lower in LEL-Fc-treated group compared to Vehicle- and hIgG1-treated groups, in IMQ induced psoriasis mouse model (Fig. 3c and Supplementary Fig. 3a). Additionally, we found that back thickness changes were significantly reduced with LEL-Fc treatment in the IMQ-treated group (Supplementary Fig. 3b). The size and weight of spleen were significantly decreased in LEL-Fc-treated mice compared to Vehicle- and hIgG1-treated groups (Fig. 3d, e). In addition, extensive epidermal hyperplasia in Vehicle- and hIgG1-treated groups was found, however, it was greatly reduced by administration of LEL-Fc in response to IMQ treatment (Fig. 3f, g). The expression of pro-inflammatory cytokines, TNF-α, IL-1β, IL-17A, and IL-6, confirmed by IHC or IF staining was higher in Vehicle- and hIgG1-treated groups, but LEL-Fc treatment dramatically suppressed their expression (Fig. 3f, g and Supplementary Fig. 4). Furthermore, LEL-Fc inhibited the IMQ-induced inflammation gene expression of *tnf-α, il-17a, il-23p19*, and *il-23p40* in mouse dorsal skin (Fig. 3h). These data indicated that LEL-Fc suppressed the psoriatic symptoms by inhibiting the expression of inflammatory cytokines.

Tm4sf19 inhibition suppressed inflammatory signaling in macrophages in IMQ-induced psoriasis mouse model

In a previous study, we demonstrated that the critical role of Tm4sf19 in macrophages in inflammatory disease. Tm4sf19 inhibition suppressed the inflammatory signaling

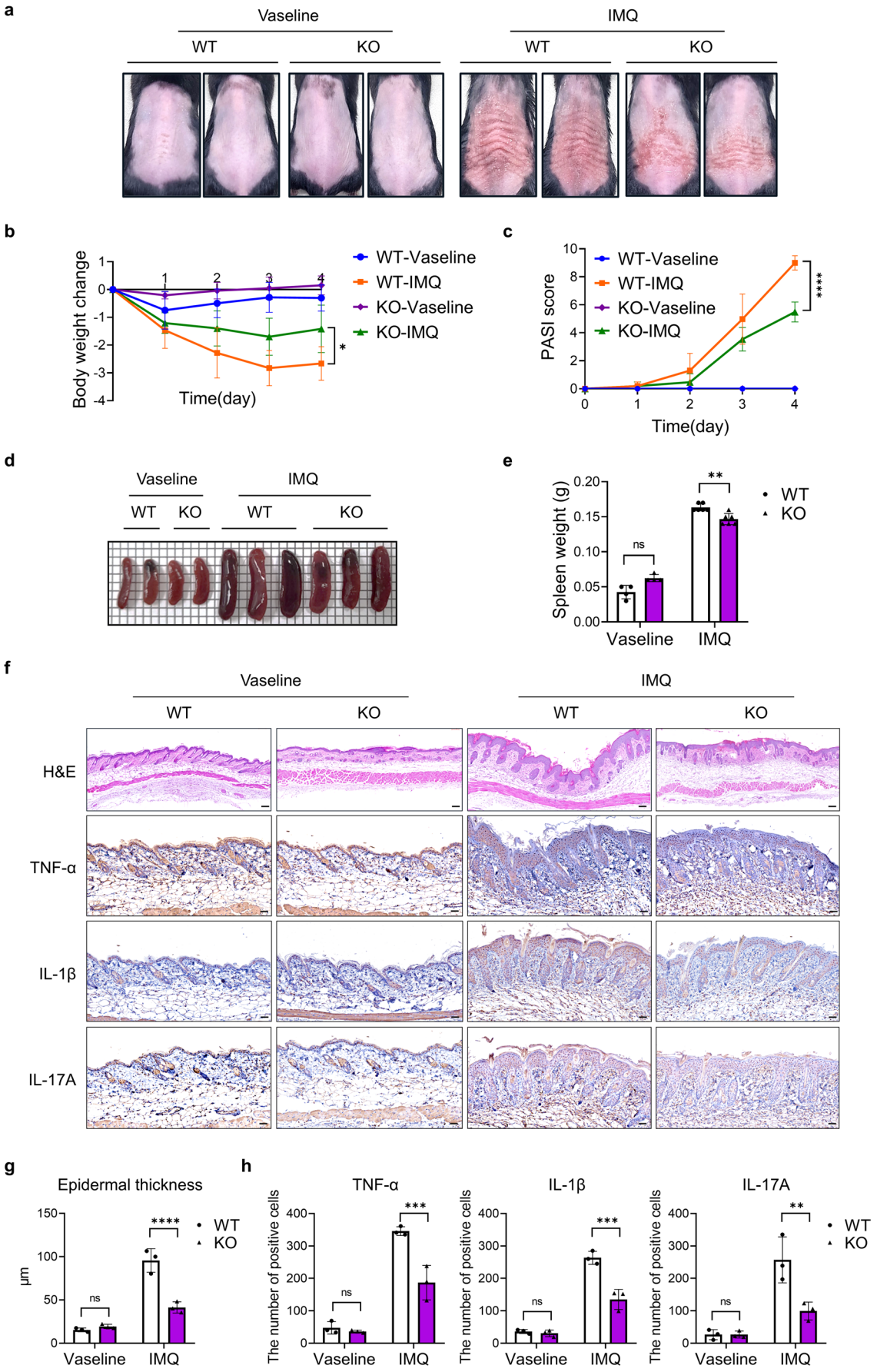
a
Vaseline
IMQ
WT
KO
WT
KO
b
Body weight change
Time(day)
WT-Vaseline
WT-IMQ
KO-Vaseline
KO-IMQ
*
c
PASI score
Time(day)
WT-Vaseline
WT-IMQ
KO-Vaseline
KO-IMQ
****
d
Vaseline
IMQ
WT
KO
WT
KO
e
Spleen weight (g)
ns
**
WT
KO
Vaseline
IMQ
f
Vaseline
IMQ
WT
KO
WT
KO
H&E
TNF-α
IL-1β
IL-17A
g
Epidermal thickness
μm
ns
****
WT
KO
Vaseline
IMQ
h
TNF-α
IL-1β
IL-17A
The number of positive cells
ns
***
**
WT
KO
Vaseline
IMQ

Fig. 2 Tm4sf19 KO reduces psoriatic skin inflammation in mice. **a** Representative image of mouse back skin from WT and KO mice treated with Vaseline or IMQ. **b, c** During IMQ treatment (b) Body weight change, (c) PASI scores. **d, e** After IMQ treatment (d) spleen size (e)spleen weight in each group. **f** H&E and IHC staining for TNF-α, IL-1β, and IL-17A in dorsal skin tissues of Vaseline- or IMQ-treated mice. Scale bar = 100 μm. **g** Quantification of epidermal thickness in f. **h** Number of TNF-α, IL-1β, or IL-17A positive cells in f. Data are expressed as mean ± SD. Data were analyzed by two-way ANOVA. $^{**}p<0.01$, $^{***}p<0.001$, $^{****}p<0.0001$

pathways in macrophages [13]. In this study, we observed that elevated expression of Tm4sf19 is mainly found in both epidermis and dermis in the dorsal skin of IMQ-treated mice (Fig. 1d). Therefore, we examined the expression of F4/80, a macrophage marker, by immunofluorescence staining. IMQ treatment increased macrophage infiltration in the dermis, and F4/80-positive macrophages were significantly reduced in the dorsal skin of KO mice compared with WT mice (Fig. 4a). Similarly, LEL-Fc treatment significantly suppressed the expression of F4/80 in the dorsal skin, thereby inhibiting macrophage activation, compared with the Vehicle-treated group following IMQ treatment (Fig. 4b). This suggests that Tm4sf19 plays an important role in promoting macrophage recruitment in the psoriatic inflammatory process [20]. The MyD88-TRAF6-NLRP3 signaling pathway mediates the innate immune response and activates Toll-like receptors (TLRs) to amplify inflammatory signals in psoriasis, leading to cytokine production and NLRP3 inflammasome activation [21–23]. IκBα, a key component of the NF-κB pathway, is known to regulate inflammatory gene transcription and maintains chronic inflammation in psoriatic lesions [24]. We confirmed that IMQ treatment increased phosphorylation of IκBα, and activated the MyD88-NLRP3 signaling pathway, a downstream signaling cascade of TLR pathway in WT mice; however, these were significantly suppressed in KO mice during IMQ treatment (Fig. 4c). Furthermore, we found that pro-inflammatory cytokines, including IL-17A, TNF-α, and IL-6, were significantly reduced in KO mice compared to WT after IMQ treatment (Fig. 4c). We further demonstrated that LEL-Fc treatment inhibited the activation of inflammatory signaling pathways, including MyD88, pIκBα, and NLRP3, and pro-inflammatory cytokines such as TNF-α and IL-6 (Supplementary Fig. 5). We also confirmed that the mRNA levels of *tnf-α*, *il-17a, il-23p19* and *il-23p40* were significantly reduced in KO mice compared to WT controls, and in LEL-Fc-treated mice compared with Vehicle-treated mice in the IMQ-induced psoriasis model (Fig. 4d, e).

To further elucidate the role of Tm4sf19 in psoriatic inflammation, we analyzed inflammatory signaling pathways in response to IMQ treatment using Tm4sf19 knockout RAW264.7 macrophages (KO#1 and KO#2), and BMDMs isolated from KO mice [13]. Phosphorylation of key inflammatory signaling proteins, including p65, p38, JNK, and ERK, was analyzed at 15 and 30 min after IMQ stimulation in RAW264.7 and BMDMs. Phosphorylation of these proteins was significantly inhibited in RAW264.7 KO#1 and KO#2 cells and Tm4sf19 KO BMDMs compared with WT, and the phosphorylation inhibition effect was more prominent at 30 min after IMQ treatment (Fig. 4f, g). Furthermore, LEL-Fc treatment significantly suppressed the phosphorylation of p65, p38, JNK, and ERK in response to IMQ in BMDMs, RAW264.7 and HaCaT cells (Fig. 4h and Supplementary Fig. 6 and 7). Tm4sf19 KO significantly reduced the mRNA expression of *il-6* and *il-23* in IMQ-treated RAW264.7 and BMDMs compared with WT cells (Fig. 4i, j). LEL-Fc treatment significantly reduced the expression of *il-6, il-1β*, and *tnf-α* induced by IMQ in RAW264.7 and BMDMs (Supplementary Fig. 8). Neutrophil infiltration is a hallmark feature of the psoriatic skin lesions [25]. We found that Tm4sf19 KO significantly suppressed neutrophil infiltration in IMQ-treated skin, as confirmed by MPO staining, a marker of neutrophil, compared to WT (Supplementary Fig. 9). In addition, administration of LEL-Fc inhibited IMQ-induced neutrophil infiltration compared to the Vehicle-treated group (Supplementary Fig. 10). These results suggest that Tm4sf19 deficiency inhibits inflammatory signaling in psoriasis by suppressing IMQ-induced macrophage activation and neutrophil infiltration and LEL-Fc is a potential therapeutic for the treatment of inflammatory dermatitis induced by activated macrophage and immune responses.

Tm4sf19 inhibition suppresses keratinocyte proliferation in psoriatic skin

In psoriasis, excessive keratinocyte proliferation is a hallmark feature that contributes to epidermal hyperplasia and the development of psoriatic plaques. This process is triggered by dysregulated signaling pathways, including EGFR, ERK, and STAT3, which amplify inflammatory responses and enhance keratinocyte activation [2]. To investigate whether Tm4sf19 modulates the EGFR signaling pathway in vivo, we analyzed the expression of EGFR and its downstream effectors in the dorsal skin of psoriatic mouse models. The expression of EGFR was significantly elevated in the psoriatic dorsal skin of WT mice. However, this increase was markedly suppressed in both Tm4sf19 KO mice and mice treated with LEL-Fc (Fig. 5a, b). Next, we evaluated the activation status of key signaling intermediates downstream of EGFR. The phosphorylation of ERK and STAT3, two major drivers of keratinocyte proliferation and inflammatory cytokine production, was significantly diminished in the Tm4sf19 KO and LEL-Fc-treated groups compared to the control group (Fig. 5a, b). To further confirm the functional

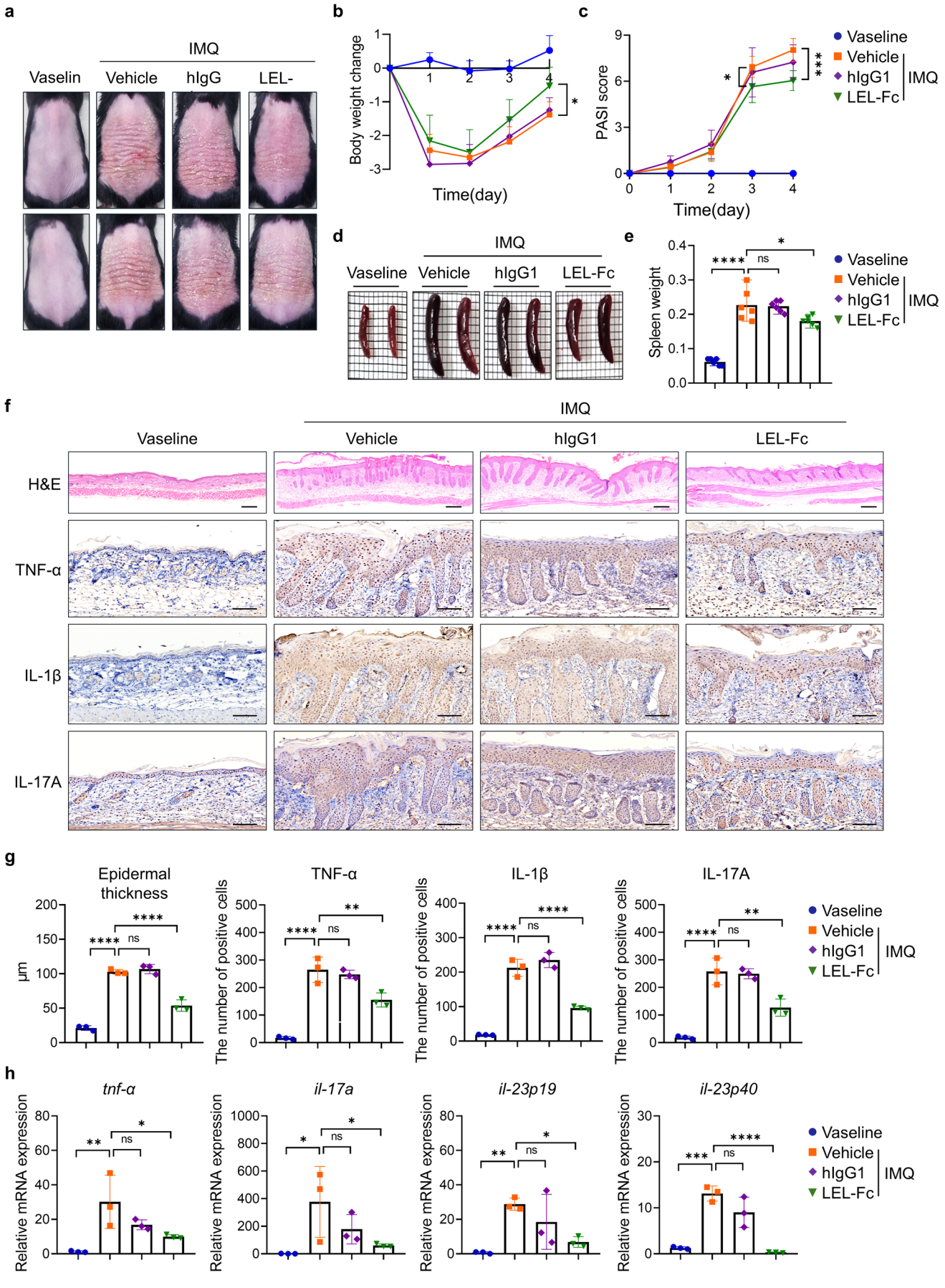
a
IMQ
Vaselin
Vehicle
hIgG
LEL-
b
Body weight change
Time(day)
c
PASI score
Time(day)
Vaseline
Vehicle
hIgG1
LEL-Fc
IMQ
d
IMQ
Vaseline
Vehicle
hIgG1
LEL-Fc
e
Spleen weight
Vaseline
Vehicle
hIgG1
LEL-Fc
IMQ
f
IMQ
Vaseline
Vehicle
hIgG1
LEL-Fc
H&E
TNF-α
IL-1β
IL-17A
g
Epidermal thickness
μm
TNF-α
IL-1β
IL-17A
The number of positive cells
Vaseline
Vehicle
hIgG1
LEL-Fc
IMQ
h
tnf-α
il-17a
il-23p19
il-23p40
Relative mRNA expression
Vaseline
Vehicle
hIgG1
LEL-Fc
IMQ

Fig. 3 LEL-Fc alleviates IMQ-induced psoriasis. **a** Representative photo of back skin from mice treated with Vehicle, hIgG1, or LEL-Fc under IMQ stimulation. **b, c** During IMQ treatment (b) Body weight change, (c) PASI scores. **d, e** After IMQ treatment (d) spleen size (e) spleen weight. **f** Representative images of H&E and IHC staining. Scale bars indicate 200 μm for H&E and 100 μm for IHC staining. **g** Quantification of epidermal thickness and TNF-α, IL-1β, or IL-17 positive cell counts in (f). **h** Relative mRNA expression analysis of maker genes in mouse back skin with Vehicle, hIgG1, or LEL-Fc under IMQ induction. Data are expressed as mean ± SD. Data were analyzed by one-way ANOVA. *$p<0.05$, **$p<0.01$, ***$p<0.001$, ****$p<0.0001$, ns = not significant

consequences of reduced EGFR signaling, we measured the expression of Keratin 17 (KRT17), a well-known downstream target of the EGFR/STAT3 pathway and a hallmark of activated keratinocytes in psoriasis. The robust induction of KRT17 observed in the psoriatic skin was effectively suppressed by Tm4sf19 inhibition (Fig. 5a, b). Consistent with these in vivo findings, we observed a similar regulatory pattern in vitro using HaCaT keratinocytes. Treatment with IMQ markedly induced the expression of EGFR, whereas LEL-Fc treatment effectively suppressed this induction and subsequently diminished the phosphorylation of ERK and STAT3 in a time-dependent manner, along with the downstream expression of KRT17 (Fig. 5c).

To further evaluate the functional impact of Tm4sf19 inhibition on epidermal pathology, we performed immunohistochemical (IHC) analysis on psoriatic dorsal skin. The results revealed that the Tm4sf19 inhibition markedly reduced the number of Ki67- and KRT17-positive proliferating keratinocytes (Fig. 5d). Furthermore, LEL-Fc treatment effectively suppressed the expression of *krt17*, indicating a reversal of the activated keratinocyte phenotype (Fig. 5e). Taken together, these findings demonstrate that Tm4sf19 promotes psoriatic phenotypes by regulating the EGFR-pERK/pSTAT3-KRT17 signaling cascade, establishing the Tm4sf19-EGFR axis as a pivotal pathogenic driver in psoriasis.

Recent studies have demonstrated that the spatial organization of EGFR within the plasma membrane as a critical determinant of its signaling efficacy. Specifically, it has been reported that tetraspanins interact with EGFR, regulate EGFR signal transduction by promoting the enrichment of signaling intermediates within specialized tetraspanin-enriched nanodomains [26]. Based on these observations, we hypothesized that Tm4sf19, a tetraspanin family protein, may functionally associate with EGFR to modulate its activation. To test this hypothesis, we examined the interaction between Tm4sf19 and EGFR using HaCaT cells expressing 3HA-hTm4sf19. Co-immunoprecipitation analysis revealed an endogenous interaction between Tm4sf19 and EGFR, and this interaction is further enhanced under inflammatory conditions, such as LPS treatment, leading to the activation of downstream pro-inflammatory cascades, whereas it was effectively attenuated upon LEL-Fc treatment (Fig. 5f). To further identify the region of Tm4sf19 responsible for its interaction with EGFR, we generated a series of Tm4sf19 deletion mutants and evaluated their binding capacity. Co-immunoprecipitation analysis revealed that the transmembrane domain 3–large extracellular loop–transmembrane domain 4 region of Tm4sf19 is essential for its interaction with EGFR (Fig. 5g, h). Consistently, a deletion mutant containing only amino acids 94–196 retained the ability to interact with EGFR, indicating that this region is sufficient for EGFR binding (Fig. 5i). These data indicated that Tm4sf19 directly associates with EGFR through a defined structural motif consisting of its transmembrane and extracellular components, which may facilitate the assembly of the Tm4sf19-EGFR signaling complex.

LEL-Fc treatment inhibits psoriasis plaque development by promoting keratinocyte apoptosis and inducing cell cycle arrest

To further elucidate the role of Tm4sf19 in keratinocyte survival, we investigated whether inhibition of Tm4sf19 promotes apoptosis in psoriasis mouse skin tissues. The number of TUNEL-positive cells was significantly increased in apoptotic keratinocytes in mouse dorsal skin of LEL-Fc-treated mice compared to Vehicle- and hIgG1-treated controls following IMQ application (Fig. 6a, b). We also confirmed that Caspase-9 expression was increased in a dose-dependent manner in HaCaT cells treated with LEL-Fc, supporting the activation of keratinocyte apoptosis (Fig. 6c). In addition, we investigated that LEL-Fc treatment significantly increased the proportion of apoptotic cells compared to mock in LPS-stimulated HaCaT cells (Fig. 6d). Next, we demonstrated that LEL-Fc treatment induced a marked cell cycle arrest compared to mock in LPS-induced HaCaT cells (Fig. 6e). The expression of *cdkn1a* and *cdkn2a*, the cyclin-dependent kinase inhibitor 1a and 2a which contribute to the stability of cell cycle arrest, was increased by LEL-Fc treatment in LPS-treated HaCaT cells (Fig. 6f). Furthermore, the expression of CDK2, CDK4 and cyclin E1, key cell cycle regulators was suppressed by LEL-Fc treatment in keratinocytes in the presence of LPS (Fig. 6g). These results suggest that LEL-Fc treatment inhibits psoriatic plaque formation by promoting apoptosis and cell cycle arrest in keratinocytes.

Discussion

Psoriasis is a chronic inflammatory skin disease that affects 2–3% of the world's population, causing significant physical, psychological, and economic burdens [27–30]. Psoriasis presents as erythematous, scaly plaques caused primarily

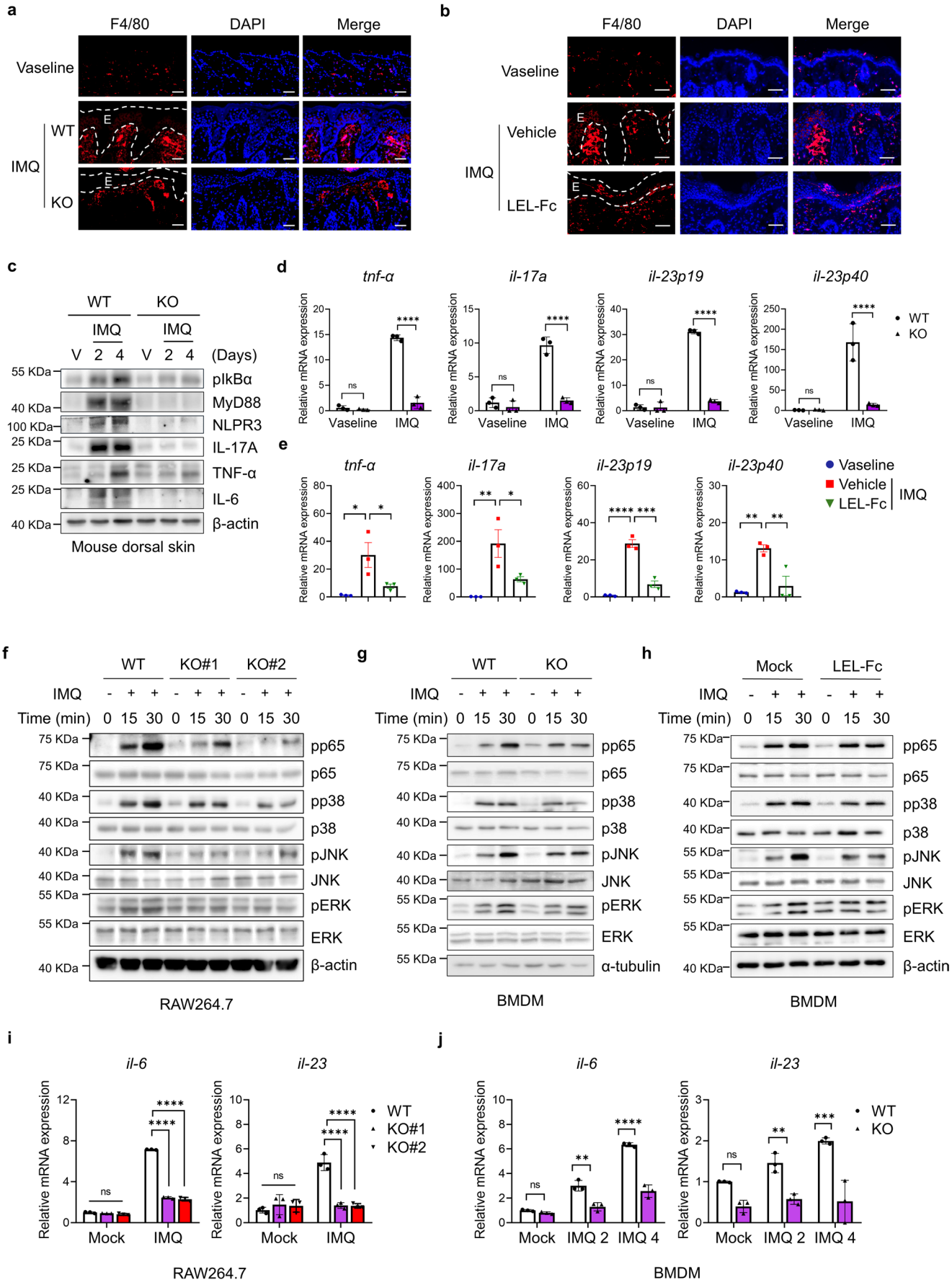
a
F4/80
DAPI
Merge
Vaseline
IMQ
WT
KO
E
b
F4/80
DAPI
Merge
Vaseline
IMQ
Vehicle
LEL-Fc
E
c
WT
KO
IMQ
V 2 4 V 2 4 (Days)
55 KDa pIkBα
40 KDa MyD88
100 KDa NLPR3
25 KDa IL-17A
25 KDa TNF-α
25 KDa IL-6
40 KDa β-actin
Mouse dorsal skin
d
tnf-α
il-17a
il-23p19
il-23p40
Relative mRNA expression
ns
****
Vaseline
IMQ
WT
KO
e
tnf-α
il-17a
il-23p19
il-23p40
Relative mRNA expression
*
**
***
****
Vaseline
Vehicle
LEL-Fc
IMQ
f
WT
KO#1
KO#2
IMQ - + + - + + - + +
Time (min) 0 15 30 0 15 30 0 15 30
75 KDa pp65
75 KDa p65
40 KDa pp38
40 KDa p38
40 KDa pJNK
40 KDa JNK
55 KDa pERK
55 KDa ERK
40 KDa β-actin
RAW264.7
g
WT
KO
IMQ - + + - + +
Time (min) 0 15 30 0 15 30
75 KDa pp65
75 KDa p65
40 KDa pp38
40 KDa p38
40 KDa pJNK
40 KDa JNK
55 KDa pERK
55 KDa ERK
55 KDa α-tubulin
BMDM
h
Mock
LEL-Fc
IMQ - + + - + +
Time (min) 0 15 30 0 15 30
75 KDa pp65
75 KDa p65
40 KDa pp38
40 KDa p38
55 KDa pJNK
55 KDa JNK
55 KDa pERK
55 KDa ERK
40 KDa β-actin
BMDM
i
il-6
il-23
Relative mRNA expression
ns
****
Mock
IMQ
WT
KO#1
KO#2
RAW264.7
j
il-6
il-23
Relative mRNA expression
ns
**
***
****
Mock
IMQ 2
IMQ 4
WT
KO
BMDM

Fig. 4 Tm4sf19 inhibition attenuates macrophage-driven inflammation. **a, b** Representative image of F4/80 immunofluorescence staining in mouse psoriatic skin tissues. The white dashed line indicates the epidermis area marked E. Scale bar = 50 μm. In psoriatic skin, **a** WT or KO **b** Vehicle-treated or LEL-Fc-treated **c** Immunoblot analysis of inflammatory mediators in mouse back skin at 2 or 4 days after IMQ treatment. **d, e** Relative mRNA expression analysis of marker genes in mouse psoriatic skin tissues of **d** WT or KO **e** Vehicle-treated or LEL-Fc-treated. **f, g, h** Western blot analysis of MAPK and NF-κB signaling in RAW264.7 KO#1 and KO#2 cells (**f**), BMDMs from (**g**) WT and KO mice (**h**) BMDMs treated with LEL-Fc after IMQ treatment. **i, j** Relative mRNA levels of *il-6* and *il-23* in (**i**) Raw 264.7 and (**j**) BMDM. IMQ 2 and IMQ 4 represent treatments with 2 and 4 μg/ml IMQ, respectively. Data are expressed as mean ± SD. Data were analyzed by two-way ANOVA. *$p < 0.05$, **$p < 0.01$, ***$p < 0.001$, ****$p < 0.0001$

by keratinocyte hyperproliferation, immune cell infiltration, and persistent inflammation. Keratinocytes contribute to disease progression by maintaining an inflammatory environment by producing cytokines and chemokines that recruit and activate immune cells [1, 2, 19, 31].

In this study, we identified Tm4sf19 as an important mediator of psoriatic inflammation. Using an IMQ-induced psoriasis mouse model, we showed that both Tm4sf19 deletion and pharmacological inhibition of Tm4sf19 markedly alleviated psoriasis-like symptoms, including epidermal hyperplasia, erythema, immune cell infiltration, and splenomegaly, accompanied by reduced levels of pro-inflammatory cytokines such as TNF-α, IL-6, IL-1β, IL-17A, and IL-23 (Figs. 2, 3). Histological analysis and PASI scores further supported the attenuation of disease severity in Tm4sf19 KO or LEL-Fc-treated mice.

The MyD88–pIκBα–NLRP3 signaling axis is well established as a key pathway in psoriasis pathogenesis, orchestrating innate immune responses and amplifying inflammatory cascades [23]. Our results showed that Tm4sf19 deficiency or LEL-Fc treatment suppressed this pathway, as evidenced by reduced expression of MyD88, pIκBα, and NLRP3 in IMQ-treated mouse skin (Fig. 4c and Supplementary Fig. 5).

Macrophages are major sources of pro-inflammatory cytokines and play an essential role in sustaining chronic inflammatory environment in psoriasis [6, 8]. We observed that both Tm4sf19 KO and LEL-Fc administration markedly reduced macrophage infiltration and suppressed NF-κB and MAPK pathway activation, leading to downregulation of *il-6*, *tnf-α*, and *il-23* (Fig. 4).

Keratinocyte hyperproliferation is a hallmark of psoriasis, driven by the upregulation of proliferation markers such as Ki-67 and KRT17, and activation of key signaling pathways including STAT3, ERK, and EGFR [32–35]. Analysis of a publicly available single-cell transcriptomic atlas of healthy and psoriatic epidermis revealed that Tm4sf19 expression is predominantly localized in keratinocyte-associated clusters (Supplementary Fig. 1) [18]. These clusters are enriched for hyperproliferative and differentiated keratinocyte populations in psoriatic lesional skin, suggesting a potential role for Tm4sf19 in keratinocyte-driven psoriatic pathology. In psoriatic skin, EGFR is overexpressed and forms signaling complexes that enhance keratinocyte proliferation and cytokine-mediated inflammation [36]. LEL-Fc treatment significantly reduced Ki-67 and KRT17 expression and suppressed EGFR-associated signaling, suggesting a pivotal role of Tm4sf19 in driving epidermal hyperplasia (Fig. 5). In addition to regulating proliferation, Tm4sf19 inhibition also promoted apoptotic regulation and cell cycle arrest in keratinocytes (Fig. 6). Our findings suggests that Tm4sf19 may facilitate these processes by interacting with EGFR, and by promoting downstream activation of STAT3 and ERK in psoriatic keratinocytes (Fig. 5).

Chronic interaction between immune cells and keratinocytes sustains the inflammatory cycle in psoriasis. Keratinocytes not only respond to inflammatory cues but also actively contribute by secreting cytokines that recruit and activate immune cells. Our findings suggest that Tm4sf19 inhibition disrupts this pathological feedback loop by suppressing keratinocyte proliferation and cytokine production, thereby attenuating immune cell infiltration and psoriatic plaque formation.

While our analysis of the GSE54456 dataset and single-cell RNA sequencing data provides supportive clinical relevance for Tm4sf19 expression in psoriatic skin, we recognize that the lack of direct validation using independent patient-derived biopsy samples represents a limitation of the present study (Fig. 1a and Supplementary Fig. 1). However, as the primary objective of this work was to elucidate the functional role of Tm4sf19 within a controlled in *vivo* murine model, further investigations involving well-characterized clinical cohorts will be essential to fully translate these mechanistic insights into human therapeutic strategies.

Currently, various therapeutic strategies are available for the treatment of psoriasis, including topical agents, systemic immunosuppressants, and biologic therapies, which primarily consist of monoclonal antibodies or fusion proteins targeting pro-inflammatory cytokines such as TNF-α, IL-17A, and IL-23. These therapies have significantly improved clinical outcomes in many patients [33, 37–40]. However, they are often limited by potential side effects, and poor long-term efficacy. These limitations highlight the need for the development of novel therapies based on alterative mechanisms of action to achieve more effective and sustained therapeutic strategies to control psoriasis [41, 42].

In conclusion, this study identifies Tm4sf19 as a critical contributor to the pathogenesis of psoriasis lesions. Inhibition of Tm4sf19 led to reduced psoriasis severity by suppressing immune cell infiltration, controlling keratinocyte proliferation, and suppressing pro-inflammatory signaling.

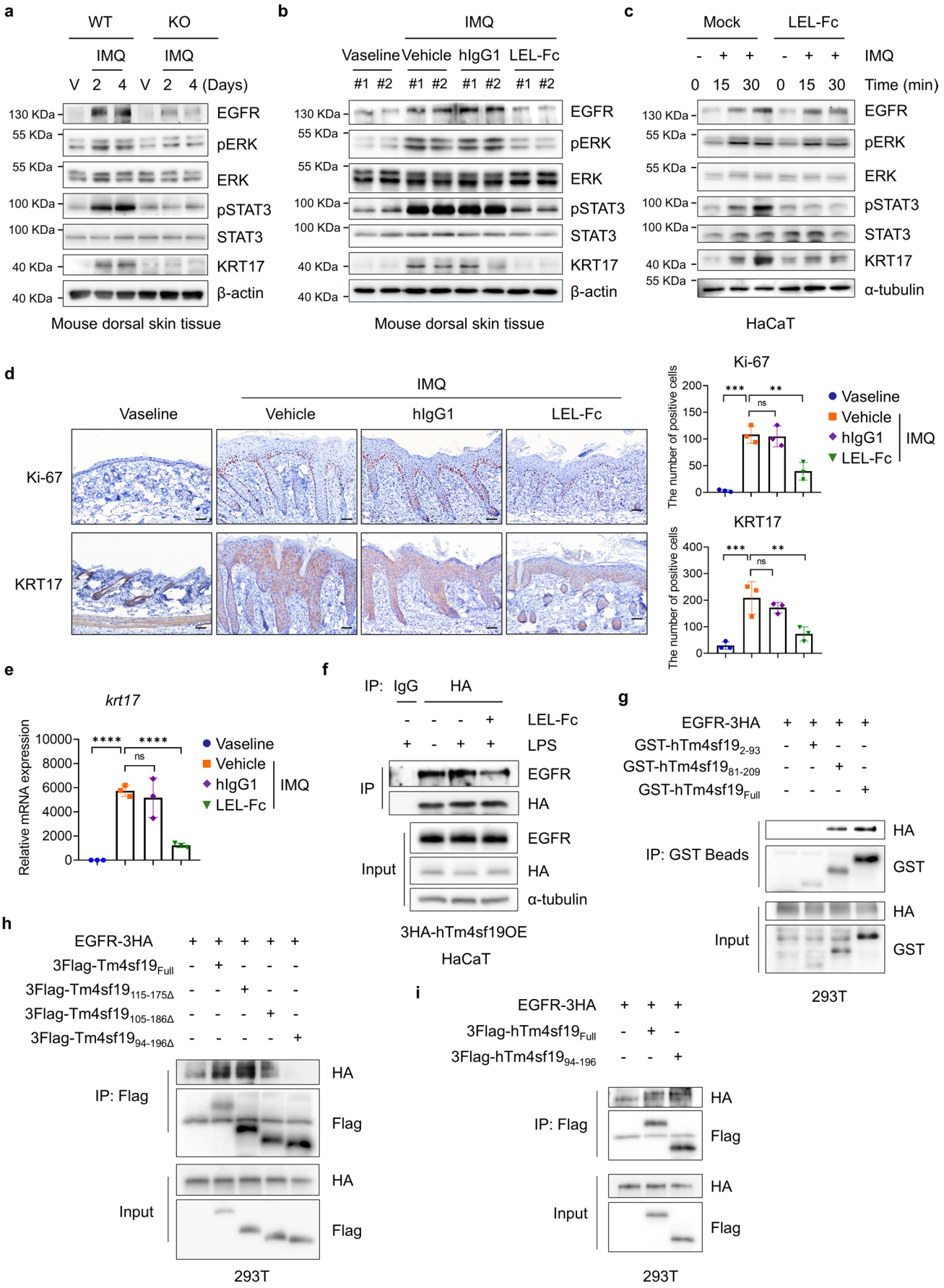
a
WT
KO
IMQ
IMQ
V 2 4 V 2 4 (Days)
130 KDa
55 KDa
55 KDa
100 KDa
100 KDa
40 KDa
40 KDa
EGFR
pERK
ERK
pSTAT3
STAT3
KRT17
β-actin
Mouse dorsal skin tissue
b
IMQ
Vaseline Vehicle hIgG1 LEL-Fc
#1 #2 #1 #2 #1 #2 #1 #2
EGFR
pERK
ERK
pSTAT3
STAT3
KRT17
β-actin
Mouse dorsal skin tissue
c
Mock
LEL-Fc
- + + - + + IMQ
0 15 30 0 15 30 Time (min)
EGFR
pERK
ERK
pSTAT3
STAT3
KRT17
α-tubulin
HaCaT
d
IMQ
Vaseline
Vehicle
hIgG1
LEL-Fc
Ki-67
KRT17
Ki-67
KRT17
The number of positive cells
***
**
ns
Vaseline
Vehicle
hIgG1
LEL-Fc
IMQ
e
krt17
Relative mRNA expression
****
****
ns
Vaseline
Vehicle
hIgG1
LEL-Fc
IMQ
f
IP: IgG HA
LEL-Fc
LPS
IP
EGFR
HA
Input
EGFR
HA
α-tubulin
3HA-hTm4sf19OE
HaCaT
g
EGFR-3HA + + + +
GST-hTm4sf19$_{2-93}$ - + - -
GST-hTm4sf19$_{81-209}$ - - + -
GST-hTm4sf19$_{Full}$ - - - +
IP: GST Beads
HA
GST
Input
HA
GST
293T
h
EGFR-3HA + + + + +
3Flag-Tm4sf19$_{Full}$ - + - - -
3Flag-Tm4sf19$_{115-175Δ}$ - - + - -
3Flag-Tm4sf19$_{105-186Δ}$ - - - + -
3Flag-Tm4sf19$_{94-196Δ}$ - - - - +
IP: Flag
HA
Flag
Input
HA
Flag
293T
i
EGFR-3HA + + +
3Flag-hTm4sf19$_{Full}$ - + -
3Flag-hTm4sf19$_{94-196}$ - - +
IP: Flag
HA
Flag
Input
HA
Flag
293T

Fig. 5 Inhibition of Tm4sf19 suppresses keratinocyte proliferation. **a, b, c** Western blot analysis of mouse dorsal skin or HaCaT cells with indicated treatments and antibodies. **a** WT or KO **b** Vaseline-, Vehicle- or LEL-Fc-treated **c** Mock or LEL-Fc-treated HaCaT cells **d** Representative image of immunohistochemistry of Ki-67 and KRT17 and quantification of Ki-67 and KRT17-positive cells in IMQ-treated mouse skin following Vehicle, hIgG1, or LEL-Fc administration. Scale bar = 50 μm. **e** Relative mRNA expression of *krt17* after indicated treatments. **f** Immunoprecipitation results showing interaction Tm4sf19 with EGFR with indicated treatment. **g, h, i** Representative immunoprecipitation results of EGFR with Tm4sf19 deletion mutants

Our findings highlight LEL-Fc as a possible therapeutic agent that targets Tm4sf19, effectively alleviating the pathogenesis of psoriasis.

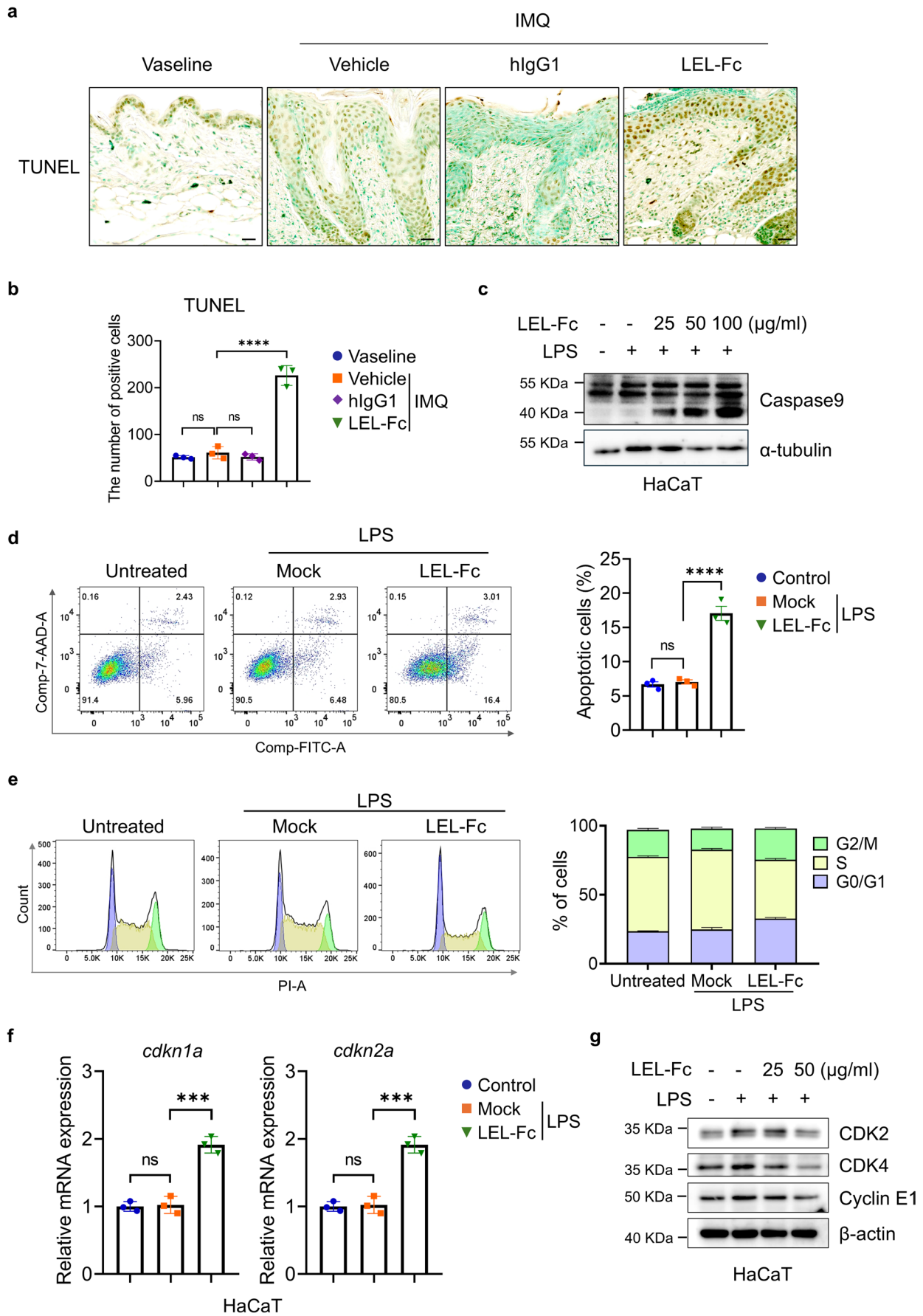
a
IMQ
Vaseline
Vehicle
hIgG1
LEL-Fc
TUNEL
b
TUNEL
The number of positive cells
300
200
100
0
****
ns
ns
Vaseline
Vehicle
hIgG1
LEL-Fc
IMQ
c
LEL-Fc - - 25 50 100 (μg/ml)
LPS - + + + +
55 KDa
40 KDa
55 KDa
Caspase9
α-tubulin
HaCaT
d
LPS
Untreated
Mock
LEL-Fc
Comp-7-AAD-A
Comp-FITC-A
0.16
2.43
91.4
5.96
0.12
2.93
90.5
6.48
0.15
3.01
80.5
16.4
Apoptotic cells (%)
25
20
15
10
5
0
****
ns
Control
Mock
LEL-Fc
LPS
e
LPS
Untreated
Mock
LEL-Fc
Count
PI-A
% of cells
100
50
0
G2/M
S
G0/G1
Untreated
Mock
LEL-Fc
LPS
f
cdkn1a
cdkn2a
Relative mRNA expression
3
2
1
0
***
ns
Control
Mock
LEL-Fc
LPS
HaCaT
g
LEL-Fc - - 25 50 (μg/ml)
LPS - + + +
35 KDa
35 KDa
50 KDa
40 KDa
CDK2
CDK4
Cyclin E1
β-actin
HaCaT

Fig. 6 LEL-Fc treatment increases apoptotic cell death, and induces cell cycle arrest. **a** Representative image of TUNEL staining. **b** quantification of TUNEL-positive cells in mouse dorsal skin with indicated treatment. Scale bar = 50 μm. **c** Western blot analysis of Caspase-9 in HaCaT cells with indicated treatment. **d** Flow cytometry analysis and quantification of apoptotic cells with indicated treatment. **e** Flow cytometry analysis of cell cycle distribution and quantification with indicated treatments. **f** Relative expression of *cdkn1a* and *cdkn2a* after indicated treatment. Data are expressed as mean ± SD. Data were analyzed by one-way ANOVA. $^{**}p<0.01$, $^{***}p<0.001$, $^{****}p<0.0001$, ns = not significant. **g** Western blot analysis of CDK2, CDK4 in LEL-Fc-treated HaCaT cells in response to LPSaa

Supplementary Information The online version contains supplementary material available at https://doi.org/10.1007/s00011-026-02245-2.

Acknowledgements This work is in part supported by GILO Foundation. We thank J. Jang, B. Choi, S. Kim and J. Ahn for Fc protein production, J. Lee, J. Jung and Y. Na for technical assistance in animal studies.

Author contributions Min Gi Kang, Sujin Park and Seong-Jin Kim conceived and designed the study. Min Gi Kang, Sujin Park, Eunji Hong, Da Seul Jung, Jin Sun Heo, and Haein An performed the experiments, collected the data and analyzed the results. Min-Jung Lee and Naim Park performed histological analysis. Min Woo Kim and Seiya Mizuno provided resources. Eunji Hong, Min Gi Kang and Sujin Park performed FACS analysis. Da Seul Jung, Hyeyeon Park, Pyunggang Kim, Minjung Son, Kyoungwha Pang, Jinah Park and Gaeun Whang contributed the formal analysis. Min Gi Kang, Sujin Park and Seong-Jin Kim wrote the first draft of the paper and Sujin Park, Eunji Hong, Yong Jung Kwon, Seiya Mizuno, Satoru Takahashi, Seok Hee Park and Seong-Jin Kim edited the paper. All authors reviewed and approved the final manuscript.

Funding No funding was received for this study.

Data availability No datasets were generated or analyzed during this study.

Declarations

Conflict of interest S.J.K. is the founder of Medpacto and serves on its Board of Directors. M.J.L., M.W.K., N. P., and S.J.K. are employees of Medpacto. The GILO Foundation has received research support from Medpacto. The other authors declare no competing interests.

References

1. Kamata M, Tada Y. Crosstalk: keratinocytes and immune cells in psoriasis. Front Immunol. 2023;14:1286344.
2. Zhou X, Chen Y, Cui L, Shi Y, Guo C. Advances in the pathogenesis of psoriasis: from keratinocyte perspective. Cell Death Dis. 2022;13(1):81.
3. Zhang Y, Shi Y, Lin J, Li X, Yang B, Zhou J. Immune cell infiltration analysis demonstrates excessive mast cell activation in psoriasis. Front Immunol. 2021;12:773280.
4. Vicic M, Kastelan M, Brajac I, Sotosek V, Massari LP. Current concepts of psoriasis immunopathogenesis. Int J Mol Sci. 2021. https://doi.org/10.3390/ijms222111574.
5. Lowes MA, Suárez-Fariñas M, Krueger JG. Immunology of psoriasis. Annu Rev Immunol. 2014;32:227–55.
6. Kamata M, Tada Y. Dendritic cells and macrophages in the pathogenesis of psoriasis. Front Immunol. 2022;13:941071.
7. Nazimek K, Bryniarski K. Macrophage functions in psoriasis: lessons from mouse models. Int J Mol Sci. 2024. https://doi.org/10.3390/ijms25105306.
8. Xia T, Fu S, Yang R, Yang K, Lei W, Yang Y, et al. Advances in the study of macrophage polarization in inflammatory immune skin diseases. J Inflamm Lond. 2023;20(1):33.
9. Hemler ME. Tetraspanin functions and associated microdomains. Nat Rev Mol Cell Biol. 2005;6(10):801–11.
10. Wright MD, Tomlinson MG. The ins and outs of the transmembrane 4 superfamily. Immunol Today. 1994;15(12):588–94.
11. Yanez-Mo M, Barreiro O, Gordon-Alonso M, Sala-Valdes M, Sanchez-Madrid F. Tetraspanin-enriched microdomains: a functional unit in cell plasma membranes. Trends Cell Biol. 2009;19(9):434–46.
12. van Deventer SJ, Dunlock VE, van Spriel AB. Molecular interactions shaping the tetraspanin web. Biochem Soc Trans. 2017;45(3):741–50.
13. Park S, Yoon K, Hong E, Kim MW, Kang MG, Mizuno S, et al. Tm4sf19 inhibition ameliorates inflammation and bone destruction in collagen-induced arthritis by suppressing TLR4-mediated inflammatory signaling and abnormal osteoclast activation. Bone Res. 2025;13(1):40.
14. Park S, Heo JS, Mizuno S, Kim M, An H, Hong E, et al. Tm4sf19 deficiency inhibits osteoclast multinucleation and prevents bone loss. Metabolism. 2024;151:155746.
15. Tsoi LC, Iyer MK, Stuart PE, Swindell WR, Gudjonsson JE, Tejasvi T, et al. Analysis of long non-coding RNAs highlights tissue-specific expression patterns and epigenetic profiles in normal and psoriatic skin. Genome Biol. 2015;16(1):24.
16. Liang Y, Tsoi LC, Xing X, Beamer MA, Swindell WR, Sarkar MK, et al. A gene network regulated by the transcription factor VGLL3 as a promoter of sex-biased autoimmune diseases. Nat Immunol. 2017;18(2):152–60.
17. Rioux G, Turgeon F, Le-Bel G, Grenier C, Guerin SL, Pouliot R. Gene profiling of a 3D psoriatic skin model enriched in T cells: downregulation of PTPRM promotes keratinocyte proliferation through excessive ERK1/2 signaling. Cells. 2022. https://doi.org/10.3390/cells11182904.
18. Gao Y, Na M, Yao X, Li C, Li L, Yang G, et al. Integrative single-cell transcriptomic investigation unveils long non-coding RNAs associated with localized cellular inflammation in psoriasis. Front Immunol. 2023;14:1265517.
19. Oji V, Luger TA. The skin in psoriasis: assessment and challenges. Clin Exp Rheumatol. 2015;33(5 Suppl 93):S14–9.
20. Tan RZ, Zhong X, Han RY, Xie KH, Jia J, Yang Y, et al. Macrophages mediate psoriasis via Mincle-dependent mechanism in mice. Cell Death Discov. 2023;9(1):140.
21. Swanson KV, Deng M, Ting JP. The NLRP3 inflammasome: molecular activation and regulation to therapeutics. Nat Rev Immunol. 2019;19(8):477–89.
22. Matsumoto R, Dainichi T, Tsuchiya S, Nomura T, Kitoh A, Hayden MS, et al. Epithelial TRAF6 drives IL-17-mediated psoriatic inflammation. JCI Insight. 2018. https://doi.org/10.1172/jci.insight.121175.
23. Costa S, Marini O, Bevilacqua D, DeFranco AL, Hou B, Lonardi S, et al. Role of MyD88 signaling in the imiquimod-induced mouse model of psoriasis: focus on innate myeloid cells. J Leukoc Biol. 2017;102(3):791–803.
24. Kawasaki T, Kawai T. Toll-like receptor signaling pathways. Front Immunol. 2014;5:461.
25. Chiang CC, Cheng WJ, Korinek M, Lin CY, Hwang TL. Neutrophils in psoriasis. Front Immunol. 2019;10:2376.

26. Sugiyama MG, Brown AI, Vega-Lugo J, Borges JP, Scott AM, Jaqaman K, et al. Confinement of unliganded EGFR by tetraspanin nanodomains gates EGFR ligand binding and signaling. Nat Commun. 2023;14(1):2681.
27. Lebwohl M. Psoriasis. Lancet. 2003;361(9364):1197–204.
28. Mahe E. Childhood psoriasis. Eur J Dermatol. 2016;26(6):537–48.
29. Griffiths CEM, Armstrong AW, Gudjonsson JE, Barker J. Psoriasis. Lancet. 2021;397(10281):1301–15.
30. Yan D, Gudjonsson JE, Le S, Maverakis E, Plazyo O, Ritchlin C, et al. New frontiers in psoriatic disease research, Part I: genetics, environmental triggers, immunology, pathophysiology, and precision medicine. J Invest Dermatol. 2021;141(9):2112-22 e3.
31. Korman NJ. Management of psoriasis as a systemic disease: what is the evidence? Br J Dermatol. 2020;182(4):840–8.
32. Shi X, Jin L, Dang E, Chang T, Feng Z, Liu Y, et al. IL-17A upregulates keratin 17 expression in keratinocytes through STAT1- and STAT3-dependent mechanisms. J Invest Dermatol. 2011;131(12):2401–8.
33. Fu M, Wang G. Keratin 17 as a therapeutic target for the treatment of psoriasis. J Dermatol Sci. 2012;67(3):161–5.
34. Luo Y, Pang B, Hao J, Li Q, Qiao P, Zhang C, et al. Keratin 17 covalently binds to alpha-enolase and exacerbates proliferation of keratinocytes in psoriasis. Int J Biol Sci. 2023;19(11):3395–411.
35. Zhang W, Dang E, Shi X, Jin L, Feng Z, Hu L, et al. The pro-inflammatory cytokine IL-22 up-regulates keratin 17 expression in keratinocytes via STAT3 and ERK1/2. PLoS ONE. 2012;7(7):e40797.
36. Wang S, Zhang Z, Peng H, Zeng K. Recent advances on the roles of epidermal growth factor receptor in psoriasis. Am J Transl Res. 2019;11(2):520–8.
37. Hawkes JE, Yan BY, Chan TC, Krueger JG. Discovery of the IL-23/IL-17 signaling pathway and the treatment of psoriasis. J Immunol. 2018;201(6):1605–13.
38. Martin DA, Towne JE, Kricorian G, Klekotka P, Gudjonsson JE, Krueger JG, et al. The emerging role of IL-17 in the pathogenesis of psoriasis: preclinical and clinical findings. J Invest Dermatol. 2013;133(1):17–26.
39. Armstrong AW, Read C. Pathophysiology, clinical presentation, and treatment of psoriasis: a review. JAMA. 2020;323(19):1945–60.
40. Ghoreschi K, Balato A, Enerback C, Sabat R. Therapeutics targeting the IL-23 and IL-17 pathway in psoriasis. Lancet. 2021;397(10275):754–66.
41. Lee HJ, Kim M. Challenges and future trends in the treatment of psoriasis. Int J Mol Sci. 2023. https://doi.org/10.3390/ijms24173313.
42. Vide J, Magina S. Moderate to severe psoriasis treatment challenges through the era of biological drugs. An Bras Dermatol. 2017;92(5):668–74.